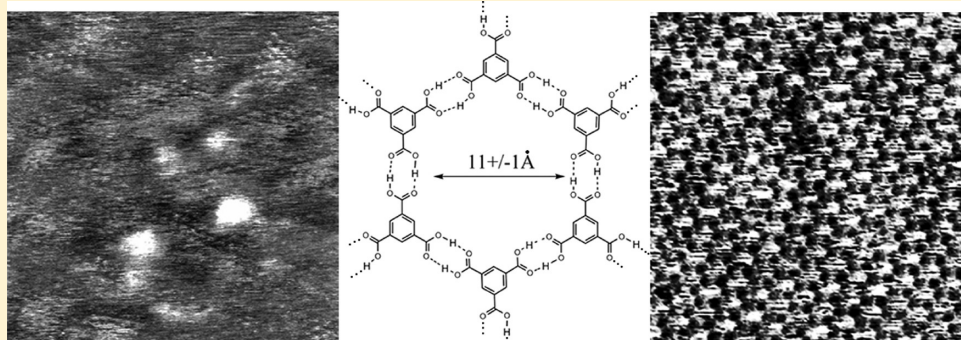


Green Chemistry Approach to Surface Decoration: Trimesic Acid Self-Assembly on HOPG

Vladimir V. Korolkov, Stephanie Allen, Clive J. Roberts, and Saul J. B. Tendler*

Laboratory of Biophysics and Surface Analysis, School of Pharmacy, The University of Nottingham, Nottingham, NG7 2RD, United Kingdom

Supporting Information



ABSTRACT: We have investigated trimesic acid (1,3,5-benzenetricarboxylic acid, TMA) adsorption on highly oriented pyrolytic graphite (HOPG) surface from aqueous medium at room temperature. Both atomic force microscopy and scanning tunneling microscopy were utilized to follow the adsorption dynamics and molecular arrangements. We have proposed an optimized green chemistry approach for fabricating trimesic acid monolayer structures on HOPG. A chicken-wire arrangement for adsorbed molecules with an average pore size of $11 \pm 1 \text{ \AA}$ was established and was observed using both scanning techniques. This structure was found to be stable in the ambient for at least two days.

The chemical decoration of surfaces with various molecules and supramolecular structures is a major strategy for introducing new properties to both organic and inorganic materials. Among these properties are wettability, biocompatibility, sensing properties, catalytic activity, optical properties, and adhesion. Most methods for surface modification include binding molecules to the surface via covalent chemical bonds. However, recently, physically adsorbed porous molecular structures (2D networks) on atomically flat surfaces have attracted attention.¹ This interest is partly due to the possible similarity in the electronic properties of 2D networks, especially covalent-bonded ones, with those of graphene-like materials.² Hence, considerable efforts have been put into fabricating similar materials with two-dimensional (2D) molecular networks being a top priority.^{1,3–5} These are usually made of two types of molecules serving two fundamental functions: joints and ribbons. 2D networks offer a unique surface property: a spatially controlled surface masking which then facilitates further molecule adsorption with extremely high spatial precision.^{6–8}

To date, the organization and detailed structure of most networks has been studied using scanning tunneling microscopy (STM) (both in ambient and ultrahigh vacuum (UHV) conditions) on metal substrates^{9–16} and highly oriented pyrolytic graphite (HOPG).^{17–20} The preparation of networks typically requires either UHV or solution-based techniques.^{8,15}

Although UHV based techniques usually present a clean and controllable route to fabricating mono/multilayers on surfaces, they are limited to specialized laboratories and cannot be easily and cheaply scaled to meet possible industrial demands. In this regard, solution-based methods represent a more likely route to success because of their relative simplicity, scalability, and cost effectiveness. However, to date, most published solution-based techniques involve formation of macromolecular structures on a surface from saturated solutions or suspensions. Such approaches do not provide effective control over the layer structure or surface coverage, both key factors in reproducibility and scale-up. Often, the choice of solvent is dictated by the needs of corresponding STM experiments (e.g., low electrical conductivity) rather than being optimal for deposition. As a result, the solvents used have been limited to phenyl octane and alkanoic acids.¹⁵ These have poor compatibility with standard molecular building blocks resulting in either oversaturated solutions or even suspensions, hence, further complicating the fabrication process as the precise concentration is not often known. These solvents are also not compatible with the growing demand for sustainable green technologies and manufacture.

Received: December 22, 2011

Revised: April 26, 2012

Published: May 2, 2012



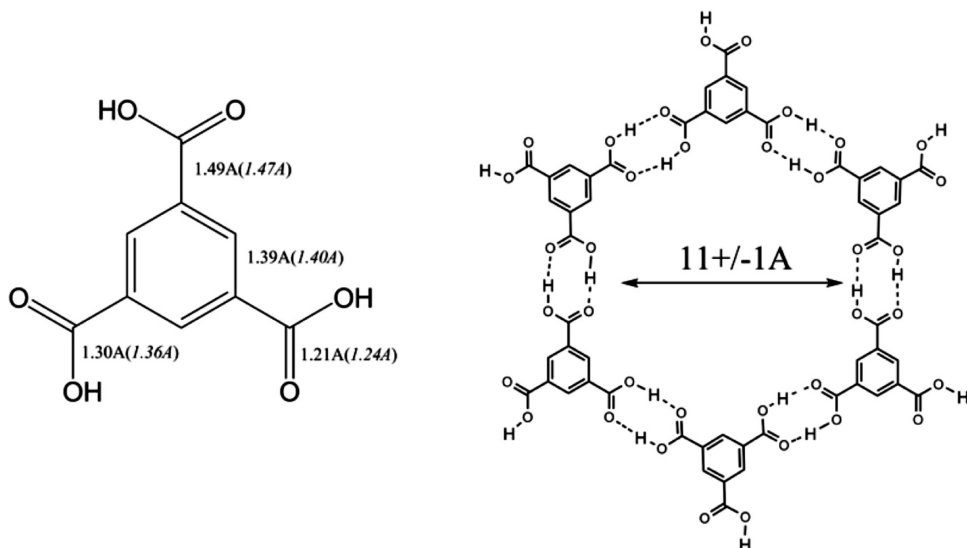


Figure 1. Molecular structure of trimesic acid and corresponding structural motif of chicken-wire network. The average pore size is $11 \pm 1 \text{ \AA}$.

Here, we propose and investigate a facile green chemistry protocol for molecular network fabrication on highly oriented pyrolytic graphite (HOPG) surfaces from water at room temperature. Trimesic acid (TMA) was chosen as a test molecular building block for our study. Both ambient STM and atomic force microscopy (AFM) were used to follow the supramolecular structure evolution over time on the HOPG surface.

Previously, TMA self-assembly was studied with STM (both in UHV and in the ambient) on several substrates: Au,^{21–24} Cu,^{25,26} Ag,²⁷ Si,²⁸ and HOPG.^{29–32} None of these studies, however, focused on the dynamics of TMA adsorption nor did they address the problem of mono/multilayers on the surfaces. In this study, we will address both the dynamics of the process and the resultant 2D structures formed on the HOPG.

■ EXPERIMENTAL SECTION

TMA (95%) was purchased from Sigma-Aldrich (Poole, United Kingdom) and was used without further purification. HOPG was purchased from NT-MDT (Zelenograd, Russia). TMA adsorption was carried out by exposing a freshly cleaved graphite surface to TMA solution in ddH₂O. In this study, we have used a standard set of TMA concentration in ddH₂O: 1, 0.1, and 0.01 mg/mL (47.6 μM). The HOPG surface was exposed to the above solutions for ~1, 10, 60, and 100 s. An HOPG sample was immersed and immediately was taken out of TMA solution with instant exposure to N₂-stream to achieve 1 s exposure. The sample was then dried in a N₂-stream for ~1 min. AFM imaging was performed with Multimode 8 scanning probe microscope with NanoScope V controller in Peak Force tapping mode (Bruker Nano). Standard Multi75Al tips (Budget Sensors, Sofia, Bulgaria) were used for imaging in ambient conditions. A set of 10 tips was calibrated to obtain accurate nanomechanical information (adhesion) from samples.

Both deflection sensitivity and spring constant (using thermal tuning method) were calibrated as described in PeakForce User Guide.³³ The averaged calibrated values for the tip are: spring constant, -2.84 N/m ; sensitivity, -67.62 nm/V .

The adhesion channel image in Peak Force tapping mode represents a distribution of peak force values below the baseline

for the force curves taken at each pixel. Hence, the adhesion channel precisely matches the height channel in terms of spatial resolution.

The TMA/HOPG sample was also imaged using an Agilent Technologies STM (Santa Clara, CA). STM tips were made by mechanically cutting Pt/Ir (20% Ir) wire (ADVENT, Research Materials Ltd., Oxford, U.K.). Imaging was performed in constant current mode with a tunneling current (I) 5–10 pA and a bias voltage (V) 500–600 mV. All presented STM images were extracted from raw data files using WSxM 5.0 program (Nanotec Electrónica, Madrid, Spain) and have not been manipulated.

■ RESULTS AND DISCUSSION

A single trimesic acid molecule has a planar structure with all three carboxylic groups coplanar with aromatic ring (Figure 1). Its crystal structure has been thoroughly investigated with X-ray diffraction techniques^{34,35} as well as estimated by ab initio methods (the structure was optimized with PC GAMMES³⁶). The experimental and calculated values are presented together with the molecule structure (Figure 1) and are in agreement. Once TMA molecules are organized in a crystal, a system of hydrogen bonds forms which stabilizes the whole structure. Previously, it was shown that TMA molecules assemble in a hydrogen-bonded 2D network within the crystal.³³ Moreover, holes/pores in this network can accommodate guest molecules such as water³⁴ and picric acid³⁴ forming a cocrystal structure. These 2D networks interpenetrate each other forming a complex 3D crystalline structure. In the crystal structure, multiple hydrogen bonds connect one network array to another leading to folded network sheets. This results in twisted and slightly tilted carboxylic groups in the TMA molecules.³³ The largest twist for COOH group around the C–C bond reaches almost 27°. Through introducing molecules to a surface, the possibility to form interpenetrated network structure is removed. Hence, they assemble in a 2D network only.

AFM Results: Adsorption Dynamics. Here, we investigate the evolution of TMA surface coverage on an underlying HOPG substrate over 100 s following the surface exposure to a TMA solution in water at room temperature. The combination of 1 mg/mL (4.8 mM) concentration and 60 s exposure time

was chosen as a starting point for our study. The starting concentration was chosen within the 1–10 mM range often used in self-assembled monolayer preparation. Sample inspection with topography and adhesion mapping AFM immediately after such exposure revealed that the HOPG surface was fully covered with multiple molecular layers (Figure 2). As the adhesion channel represents the interaction between

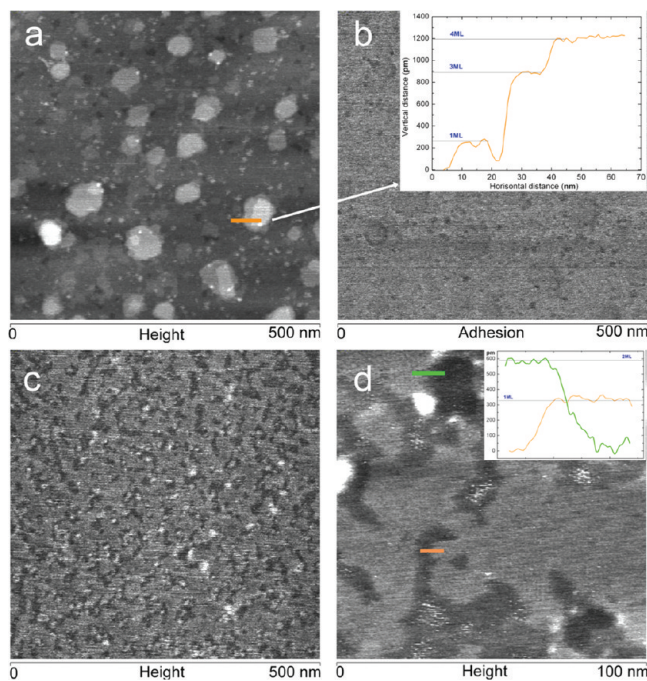


Figure 2. (a, b) AFM images (height and adhesion channels) showing multilayered structure for TMA on HOPG (adsorption time, 1 min; concentration, 1 mg/mL). An inset shows a cross section showing a stack of monolayers. (c, d) AFM height images showing a multilayered structure for TMA on HOPG (adsorption time, 1 s; concentration, 1 mg/mL). An inset shows mono and double layers.

the tip and the surface, it is influenced by the chemical nature of the underlying layers; this helps to distinguish TMA from bare HOPG substrate. However, the quantitative interpretation of adhesion values is not straightforward as the tip chemistry and the geometry of tip–surface interaction/contact are not always well-defined or comparable from tip to tip. Nevertheless, the adhesion data does reliably distinguish between the TMA and HOPG and provides additional structural information to the height channel.

Figure 2 presents AFM image data showing a TMA multilayer structure on HOPG. Dark patches (dark areas on the AFM height image) in the layers represent views of the underlying TMA layer. Careful inspection of the corresponding height cross sections reveals that the average depth of each layer is ~0.3 nm. This matches with the expectations of the thickness of a single molecular layer. The inset in Figure 2b clearly shows four such monolayers with distinctive steps (~0.3 nm). Patch sizes do not exceed ~15 nm in diameter. The corresponding adhesion map shows fairly uniform adhesion distribution across the sample indicating chemical homogeneity and, hence, complete coverage of the HOPG by the TMA. The slight contrast in adhesion on the patch borders may represent adhesion differences because of the chemistry exposed at the step edges but may also result from changes in contact area with the AFM tip that occur at step edges. Hence, under these

conditions, the AFM indicates full TMA surface coverage with some areas covered by stacks (bright areas on the AFM height image) of 3–5 molecular layers with the upper TMA layers showing incomplete coverage with small gaps evident (~5–15 nm in diameter). The diameter for these stacks did not exceed ~50 nm on average.

To reduce the amount of TMA deposited, the exposure time was reduced to ~1 s keeping the concentration the same (1 mg/mL). AFM images (500 nm × 500 nm and 100 nm × 100 nm) are presented in Figure 2 (c and d). The obvious difference between Figure 2a and 2c, d is the lack of multilayered stacks. Clearly, the drop in exposure time has resulted in a smooth layered structure. The average cross section (Figure 2d, shown in orange) shows that the topmost layer is a monolayer with a typical thickness of 0.3 nm. We also observed 0.6 nm steps (Figure 2d, shown in green) which clearly suggest a double-layer structure. The analysis of the corresponding adhesion map (Supporting Information) again indicates a chemically homogeneous surface and, hence, full surface coverage of TMA, although we note small (~5–10 nm in diameter) spots with lower (by ~150 pN) adhesion compared to the rest of the image. These spots correspond to features of the same size in the height image. At this time, we cannot draw a solid and unambiguous conclusion about their nature because of the inconsistency in their heights and shapes across the image: they might well represent areas with disoriented molecules or some complex supramolecular structures.

To investigate the effect of TMA concentration, it was reduced to 0.1 mg/mL with the same adsorption time of ~1 s as shown in Figure 3: AFM analysis revealed that the HOPG

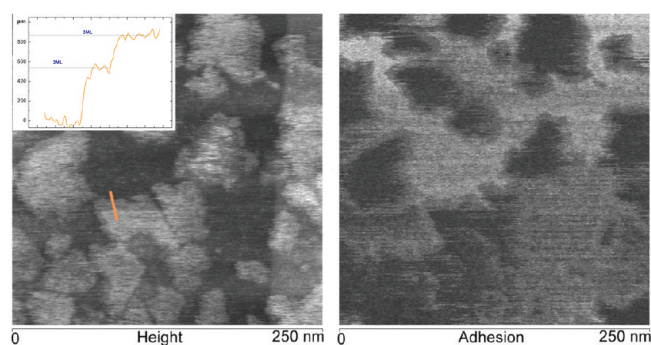


Figure 3. AFM images (height and adhesion channels) showing a multilayered structure for TMA on HOPG (adsorption time, 1 s; concentration, 0.1 mg/mL). A stack of three monolayers is presented in the inset.

surface was covered with stacks of 2–3 monolayers of TMA. Their dimensions as measured from the image do not exceed ~100 nm on average. The most striking difference comes from the comparison of adhesion maps. For this sample, the adhesion map consists of areas with different adhesion which precisely match dimensions of monolayer stacks on the height image (Figure 3). Monolayer stacks appear as dark areas on the adhesion map. Thus, it would be reasonable to conclude that for this sample we observe both the HOPG bare surface and the TMA monolayers organized in stacks. This conclusion is supported by a visual comparison of the monolayer structure with surrounding uncovered areas in the topography. The adhesion values for the organic TMA are lower than for HOPG. In this example, the average difference in adhesion values is

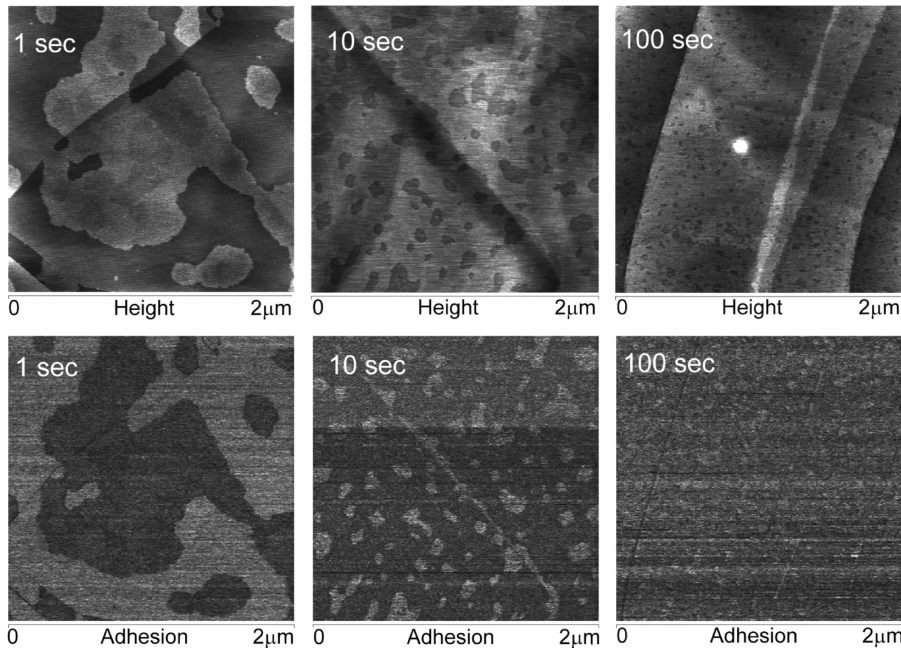


Figure 4. A set of height (upper row) and adhesion (lower row) images ($2 \mu\text{m} \times 2 \mu\text{m}$) showing TMA coverage evolution within the first 100 s of adsorption. The dark regions on the adhesion map correspond to the areas with lower adhesion. Each image represents a sample prepared at a given time and concentration of 0.01 mg/mL.

around 300 pN. The absolute adhesion value for TMA monolayer reaches 150 pN on the average (Figure 3). We found that different tips give the same absolute adhesion values which suggests that the contact area (although not known) is almost the same. Thus, we can compare absolute adhesion values at least semiquantitatively. Thus, a combination of 0.1 mg/mL concentration and 1 s adsorption time resulted in the HOPG surface only being partly covered with stacks of TMA monolayers.

A further decrease of concentration to 0.01 mg/mL and the same adsorption time of 1 s results in a submonolayer (ca. 50%) structure on the HOPG (Figure 4). The adhesion map again helps to distinguish between the TMA and the HOPG monolayer as they appear as a dark layer on a light background. The height image in Figure 4 (1 s) shows an interesting feature that the monolayer overlays an atomic step on the HOPG. This fact suggests that possible defects (various oxygen-containing groups) that usually occur on step edges do not have a serious impact on the TMA monolayer formation suggesting that high-quality HOPG with large atomically flat terraces is not a necessity for layer formation. As the adsorption time increases, the monolayer gradually saturates and reaches $\sim 90\%$ coverage within 100 s. The second layer starts to form after ~ 10 s of adsorption (Figure 4). An overview of adsorption process within the first 100 s of HOPG surface exposure is presented in Figure 4.

These studies suggest that at TMA concentrations higher than 0.1 mg/mL TMA molecules prefer forming stacks of monolayers rather than a continuous monolayer. With a lower concentration ($\sim <0.01$ mg/mL), TMA molecules first form a continuous monolayer, and then the second layer starts to form.

Molecular Arrangement: STM and AFM Analysis. Having established the dynamics of TMA monolayer formation, the precise molecule arrangement within it was examined by both AFM and STM.

STM Analysis. For the STM study, we used the same sample previously assessed with AFM and displayed in Figure 2. Molecular resolved STM scans are presented in Figure 5(a and

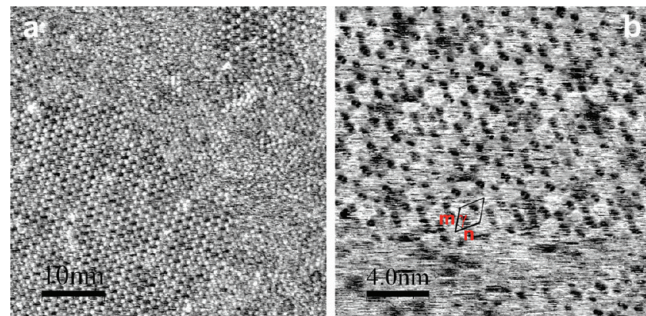


Figure 5. Ambient STM images showing TMA molecules arranged in a chicken-wire structure on HOPG (adsorption time, 1 min; concentration, 1 mg/mL). Scanning parameters are as follows: (a) $I = 5 \text{ pA}$, $U = +0.55 \text{ V}$, (b) $I = 7 \text{ pA}$, $U = +0.55 \text{ V}$. The contrast has been reversed for clarity on image b.

b). Both images show molecules arranged in a chicken-wire structure ($m = n = 16.90 \pm 0.5 \text{ \AA}$, $\gamma = 60^\circ$) where we assume that each molecule interacts with three others via hydrogen bonding. The dark round shaped features are related only to the aromatic core of the TMA molecule. Thus, STM does not detect carboxylic groups with the settings used.

The distance between centers of oppositely placed molecules is $19.2 \pm 0.5 \text{ \AA}$ which matches previously reported results for TMA single crystal ($\sim 19.3 \text{ \AA}$ calculated from distances in publication³³). The corresponding pore size is $11.0 \pm 0.5 \text{ \AA}$. Hence, the TMA chicken-wire structure represents a 2D honeycomb hydrogen-bonded network with open pores of $11.0 \pm 0.5 \text{ \AA}$ in diameter. It is clear from scan b that certain pores appear brighter than others. As the imaging is under ambient conditions, we could speculate that this may be due to trapped

water molecules in some of the pores. Scan a reveals that apart from the chicken-wire structure there is a more densely packed structure. However, it would be difficult to assign any molecular arrangement to it as it is not as well resolved as the former one. From the corresponding AFM experiment, we know that the sample structure consists of a few monolayers and that possibly this poorly resolved structure in STM is related to the multilayered areas seen in AFM. This is also consistent with the fact that stable imaging was only possible at an extremely low set point of 5–7 pA (just above the noise level which was around 2–3 pA) and a bias voltage of +0.55 V as a multilayer TMA sample might be expected to only conduct very low currents in comparison to a single monolayer. Any higher values for the set point resulted in significant image quality deterioration. Moreover, even keeping that combination of current and bias did not allow us to acquire more than 1–2 scans from the same area of the sample as discussed in more detail later.

AFM Analysis. Although STM gives precise information on molecule placement on the surface, it is extremely time-consuming to achieve the quality of images reported, and STM only provides detailed information for the first layer of TMA molecules at the HOPG interface.

Careful examination of Figure 2d already indicates the presence of a substructure within the monolayer. High-resolution AFM imaging of the monolayer structure for the same sample is presented in Figure 6 (a and b). Both height

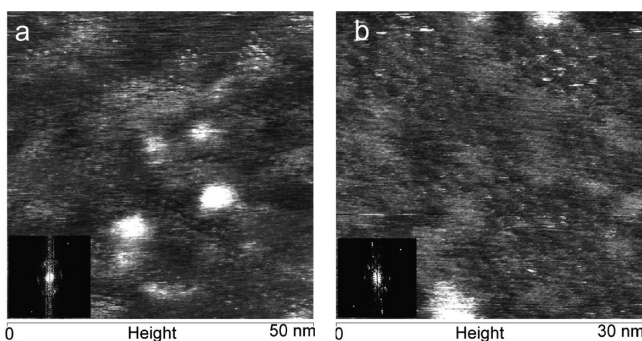


Figure 6. Highly resolved AFM images showing the chicken-wire structure for the same sample presented in Figure 2 (adsorption time, 1 min; concentration, 1 mg/mL). Both 2D-FFT insets show a periodic arrangement of structure.

images show an arrangement of hexagonal units (which appear as bright round shaped features) on the surface. The average diameter for these units is $\sim 11 \pm 2$ Å. 2D-fast Fourier

transform (FFT) insets indicate a periodicity of $\sim 16 \pm 1$ Å which agrees with the STM findings (16.9 ± 0.5 Å). Thus, we can conclude that AFM has resolved the open-pore structure of the TMA monolayer. The pores appear topographically higher than surrounding molecular units. The cause of this contrast is not clear. It may be explained by accommodation of guest molecules, such as H_2O from the ambient environment, inside the 2D porous structure. A similar conclusion has been drawn previously from analyzing the STM data presented in Figure 5.

Three further high-resolution AFM scans (Figure 7) show detail of the monolayer structure for the sample previously shown in Figure 4 (1 s). Scans a and b present information from the height channel, and scan c shows information from the adhesion channel. All scans were taken from the same area with the scan size decreasing from a to c. 2D-FFT confirms the periodic structure. A cross section from three open pores is shown in orange on scan b. An average pore size of 10.1 ± 2.4 Å and a periodicity of $\sim 16 \pm 1$ Å were measured from cross section and 2D-FFTs (for both scans a and b), respectively. These values agree with those from the multilayered sample thus indicating structural similarity between the two layers. Again, pores appear topographically higher (brighter) than the surrounding molecules, although some of them (orange cross section, scan b) do have a contrast that might be expected from geometric consideration alone. Again, such contrast behavior may result from guest H_2O molecules which when absent give the reverse contrast. Similar structural information can be extracted from the adhesion map as well (Figure 7c).

TMA Layer Stability in Ambient STM Experiment.

Images taken at 5 min intervals (Figure 8) show TMA network structure disruption followed by competitive adsorption of long-chain contaminants from the ambient. Such desorption does not necessarily mean molecules leaving the surface to the ambient as we cannot follow their fate away from the immediate surface within the scope of STM experiment. The process of desorption/competitive adsorption is relatively fast. It is unclear from the STM experiment whether the competitive adsorption process is tip mediated or not. For a similar system studied with AFM, we did not observe such behavior while imaging. Moreover, a partly covered TMA/HOPG sample left in the ambient did not show any changes when imaged with AFM immediately after preparation or following 48 h (data not shown). This suggests that AFM is a gentler tool to investigate TMA monolayers under ambient conditions.

CONCLUSIONS

A simple and straightforward protocol for TMA monolayer fabrication from aqueous media on a HOPG surface has been

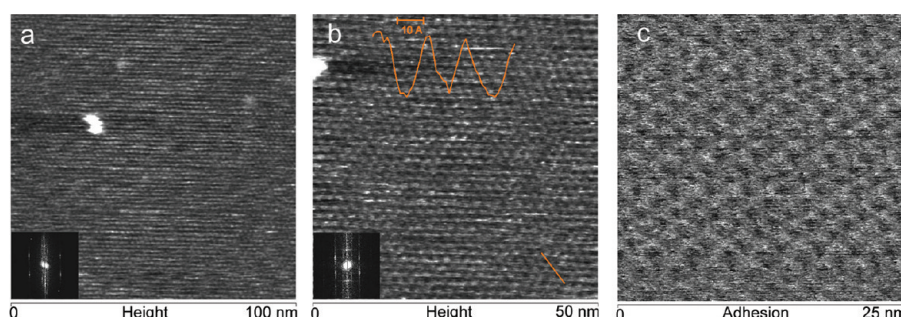


Figure 7. Highly resolved AFM images showing chicken-wire structure for the sample presented in Figure 5 (adsorption time, 1 s; concentration, 0.01 mg/mL). Both 2D-FFT insets show a periodic arrangement of TMA structure. Image C shows the adhesion distribution.

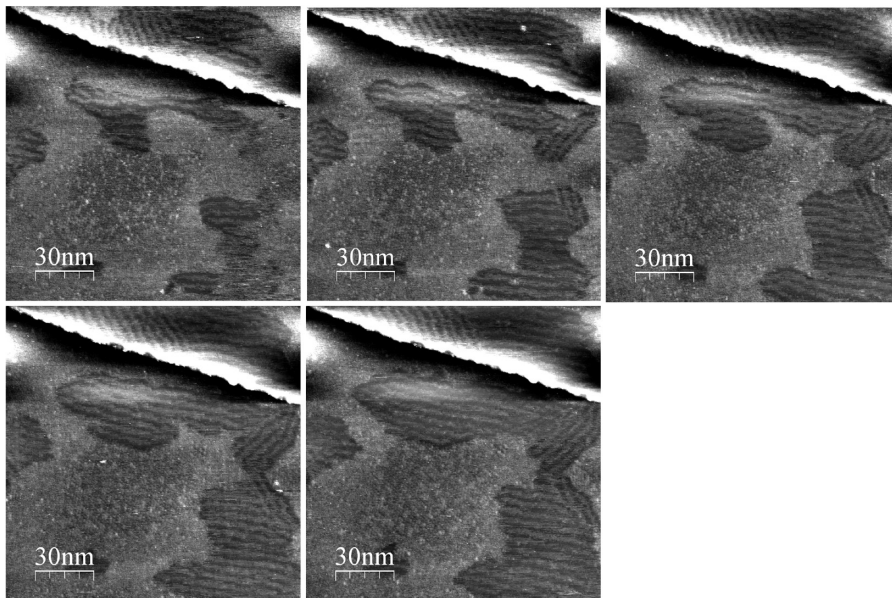


Figure 8. A set of ambient STM images showing gradual deterioration of multilayered structure for the sample presented in Figure 2 (adsorption time, 1 min; concentration, 1 mg/mL). Images are taken at 5 min intervals.

developed. TMA monolayer structure was resolved to a similar nanometer resolution with both STM and AFM. Both techniques revealed a chicken-wire structure on the surface. We found that this structure forms a monolayer within ~100 s of exposure of HOPG surface to ~50 μ M solution of TMA in H_2O . The monolayer structure was found to be stable for at least 48 h under ambient conditions. STM was observed to lead to some desorption of TMA from a dynamically formed TMA film and was only able to image the monolayer of TMA molecule in intimate contact with the HOPG. AFM revealed that TMA films with higher concentration or longer adsorption times formed multilayers with similar molecular spacing and displayed an island growth morphology. Overall, a facile green chemistry method for monolayer fabrication has been established.

■ ASSOCIATED CONTENT

S Supporting Information

An AFM adhesion map for the sample presented in Figure 2c. This material is available free of charge via the Internet at <http://pubs.acs.org>.

■ AUTHOR INFORMATION

Notes

The authors declare no competing financial interest.

■ ACKNOWLEDGMENTS

The authors would like to thank The University of Nottingham for funding this work. We thank Prof. Peter Beton, School of Physics and Astronomy, The University of Nottingham, for access to the Agilent STM.

■ REFERENCES

- (1) Bartels, L. *Nat. Chem.* **2010**, *2*, 87–95.
- (2) Novoselov, K. S.; Jiang, D.; Schedin, F.; Booth, T. J.; Khotkevich, V. V.; Morozov, S. V.; Geim, A. K. *Proc. Natl. Acad. Sci. U.S.A.* **2005**, *102* (30), 10451–10453.
- (3) Theobald, J. A.; Oxtoby, N. S.; Phillips, M. A.; Champness, N. R.; Beton, P. H. *Nature* **2003**, *424*, 1029–1031.
- (4) Pawin, G.; Wong, K. L.; Kwon, K. Y.; Bartels, L. *Science* **2006**, *313*, 961–962.
- (5) Perdigao, L. M. A.; Perkins, E. W.; Ma, J.; Staniec, P. A.; Rogers, B. L.; Champness, N. R.; Beton, P. H. *J. Phys. Chem. B* **2006**, *110*, 12539–12542.
- (6) Schlickum, U.; Decker, R.; Klappenberger, F.; Zoppellaro, G.; Klyatskaya, S.; Ruben, M.; Silanes, I.; Arnaud, A.; Kern, K.; Brune, H.; Barth, J. V. *Nano Lett.* **2007**, *7*, 3813–3817.
- (7) Stepanow, S.; Lin, N.; Barth, J. V.; Kern, K. *Chem. Commun.* **2006**, *20*, 2153–2155.
- (8) Madueno, R.; Raisanen, M. T.; Silien, C.; Buck, M. *Nature* **2008**, *454*, 618–621.
- (9) Zhang, H.-M.; Pei, Z.-K.; Xie, Z.-X.; Long, L.-S.; Mao, B.-W.; Xu, X.; Zheng, L.-S. *J. Phys. Chem. C* **2009**, *113* (31), 13940–13946.
- (10) Pawin, G.; Wong, K. L.; Kim, D.; Sun, D.; Bartels, L.; Hong, S.; Rahman, T. S.; Carp, R.; Marsella, M. *Angew. Chem., Int. Ed.* **2008**, *47*, 8442–8445.
- (11) Kuhne, D.; Klappenberger, F.; Decker, R.; Schlickum, U.; Brune, H.; Klyatskaya, S.; Ruben, M.; Barth, J. V. *J. Am. Chem. Soc.* **2009**, *131* (11), 3881–3883.
- (12) Langner, A.; Tait, S. L.; Lin, N.; Rajadurai, C.; Ruben, M.; Kern, K. *Proc. Natl. Acad. Sci. U.S.A.* **2007**, *104* (46), 17927–17930.
- (13) Dmitriev, A.; Spillmann, H.; Lin, N.; Barth, J. V.; Kern, K. *Angew. Chem., Int. Ed.* **2003**, *42*, 2670–2673.
- (14) Staniec, P. A.; Perdigao, L. M. A.; Rogers, B. L.; Champness, N. R.; Beton, P. H. *J. Phys. Chem. C* **2007**, *111*, 886–893.
- (15) Swarbrick, J. C.; Rogers, B. L.; Champness, N. R.; Beton, P. H. *J. Phys. Chem. B* **2006**, *110* (12), 6110–6114.
- (16) Perdigao, L. M. A.; Champness, N. R.; Beton, P. H. *Chem. Commun.* **2006**, 538–540.
- (17) Breitrock, A.; Hostera, H. E.; Meier, C.; Ziener, U.; Behm, R. J. *Surf. Sci.* **2007**, *601* (18), 4200–4205.
- (18) Blunt, M. O.; Russell, J. C.; Giménez-López, M. d. C.; Garrahan, J. P.; Lin, X.; Schröder, M.; Champness, N. R.; Beton, P. H. *Science* **2008**, *322* (5904), 1077–1081.
- (19) Liu, J.; Zhang, X.; Yan, H.-J.; Wang, D.; Wang, J.-Y.; Pei, J.; Wan, L.-J. *Langmuir* **2010**, *26* (11), 8195–8200.
- (20) Zhao, J.-F.; Li, Y.-B.; Lin, Z.-Q.; Xie, L.-H.; Shi, N.-E.; Wu, X.-K.; Wang, C.; Huang, W. *J. Phys. Chem. C* **2010**, *114* (21), 9931–9937.
- (21) Ishikawa, Y.; Ohira, A.; Sakata, M.; Hirayama, C.; Kunitake, M. *Chem. Commun.* **2002**, 2652–2653.
- (22) Han, B.; Li, Z.; Pronkin, S.; Wandlowski, T. *Can. J. Chem.* **2004**, *82*, 1481.

- (23) Su, G.-J.; Zhang, H.-M.; Wan, L.-J.; Bai, C.-L.; Wandlowski, T. *J. Phys. Chem. B* **2004**, *108*, 1931–1937.
- (24) Ye, Y.; Sun, W.; Wang, Y.; Shao, X.; Xu, X.; Cheng, F.; Li, J.; Wu, K. *J. Phys. Chem. C* **2007**, *111*, 10138–10141.
- (25) Dmitriev, A.; Lin, N.; Weckesser, J.; Barth, J. V.; Kern, K. *J. Phys. Chem. B* **2002**, *106*, 6907–6912.
- (26) Classen, T.; Lingenfelder, M.; Wang, Y.; Chopra, R.; Virojanadara, C.; Starke, U.; Costantini, G.; Fratesi, G.; Fabris, S.; Gironcoli, S.; et al. *J. Phys. Chem. A* **2007**, *111*, 12589–12603.
- (27) Sheerin, G.; Cafolla, A. A. *Surf. Sci.* **2005**, *577*, 211–219.
- (28) Garah, M.; Makoudi, Y.; Cherioux, F.; Duverger, E.; Palmino, F. *J. Phys. Chem. C* **2010**, *114*, 4511–4514.
- (29) Griessl, S.; Lackinger, M.; Edelwirth, M.; Hietschold, M.; Heckl, W. M. *Single Mol.* **2002**, *3* (1), 25–31.
- (30) Lackinger, M.; Griessl, S.; Heckl, W. M.; Hietschold, M.; Flynn, G. W. *Langmuir* **2005**, *21*, 4984–4988.
- (31) Nath, K. G.; Ivasenko, O.; Miwa, J. A.; Dang, H.; Wuest, J. D.; Nanci, A.; Perepichka, D. F.; Rosei, F. *J. Am. Chem. Soc.* **2006**, *128*, 4212–4213.
- (32) Ha, N. T. N.; Gopakumar, T. G.; Gutzler, R.; Lackinger, M.; Tang, H.; Hietschold, M. *J. Phys. Chem. C* **2010**, *114*, 3531–3536.
- (33) *PeakForce QNM User Guide*; Veeco Instruments Inc.: New York, 2010; pp 1–90.
- (34) Duchamp, D. J.; Marsh, R. E. *Acta Crystallogr.* **1969**, *B25*, 5–19.
- (35) Herbstein, F. H.; Marsh, R. E. *Acta Crystallogr.* **1977**, *B33*, 2358–2367.
- (36) Schmidt, M. W.; Baldridge, K. K.; Boatz, J. A.; Elbert, S. T.; Gordon, M. S.; Jensen, J. H.; Koseki, S.; Matsunaga, N.; Nguyen, K. A.; Su, S. J.; et al. *J. Comput. Chem.* **1993**, *14*, 1347–1363.